Express Polymer Letters Vol.18, No.9 (2024) 921–930
Available online at www.expresspolymlett.com
https://doi.org/10.3144/expresspolymlett.2024.69

Research article

Polypropylene blends: Impact of long chain-branched polypropylene on crystallization of linear polypropylene

*Soňa Zenzingerová, Jana Navratilova**, Lenka Gajzlerová, Michal Kudláček, David Jaška, Lubomir Benicek, Roman Čermák*

Department of Polymer Engineering, Faculty of Technology, Tomas Bata University in Zlin, Vavreckova 5669, 760 01 Zlin, Czech Republic

Received 29 May 2024; accepted in revised form 24 June 2024

Abstract. This study compares the efficiency of commercially available sorbitol-based clarifying agent (NA) and varying amounts of long chain-branched polypropylene (LCBPP) acting as a specific α-nucleating agent for linear polypropylene (PP). The sorbitol-based clarifying agent, 1,3;2,4-bis(3,4-dimethyl benzylidene)sorbitol (Millad 3988), in concentration 0.2 wt%, and LCBPP in the concentration of 1, 2, 5 and 10 wt% were mixed into PP. The comparison of the effect of NA and long branches under isothermal conditions on the crystallization process, crystallinity and polymorphic composition was realized by differential scanning calorimetry and wide-angle X-ray scattering. The addition of long chain-branched polypropylene, even at the lowest concentration, performs better at higher crystallization temperatures and has a superior effect on the crystallization process, crystallization rate and overall crystallization than the addition of NA.

Keywords: *crystallization, morphology, polyolefins, blends, crystal growth, polypropylene*

1. Introduction

Polypropylene (PP) ranks among the most commercially used polymer materials due to its low price and good technological processability. It is a highly adjustable material known for its outstanding mechanical properties, good chemical resistance, and thermal stability, making it suitable for many applications. PP is widely used in automotive, packaging, electrical engineering and healthcare. PP can be easily processed using various methods, including injection moulding, extrusion, and blow moulding, allowing a high degree of design flexibility and efficient production [1]. Commercial PP is commonly prepared using iso-specific Ziegler-Natta or metallocene catalysts, producing linear chains and, in the case of the second mentioned, narrow molecular weight distribution. The resulting linear structure of PP limits its applications for processes where good extensional properties and melt strength are required, such as thermoforming, film blowing, foaming and fibre spinning [1, 2]. An effective strategy for enhancing these constraining properties involves introducing long chains onto the polypropylene backbone [3, 4]; incorporating long-chain branching in PP significantly influences the crystallization and resultant morphology. Long-chain branched polypropylene (LCBPP) exhibits structural defects impacting nucleation and crystallite growth. In cases where LCBPP is generated through a radical-driven synthesis process utilizing peroxides in the molten state, the formation of long branches is linked to chain scission and gel formation, significantly influencing the nucleation rate. The self-seeding effect of LCBPP has been observed, underscoring its impact on crystallization [5–7].

PP exists in four crystalline structures, α-, β-, γ- and smectic structure, an intermediate between crystalline

---

*Corresponding author, e-mail: j1navratilova@utb.cz and fully amorphous phases of PP. These structures depend on crystallization conditions with the possibility of recrystallization. The monoclinic α-phase, formed under established processing conditions, can recrystallize from a less ordered α_1-phase with a random distribution of 'up' and 'down' chain packing of methyl pendant groups to a more ordered α_2-phase with a well-defined deposition of 'up' and 'down' helices in the crystal unit cell [8]. The trigonal β-phase can be induced by creating adequate crystallization conditions, such as a high-temperature gradient, the presence of shear forces, or the most efficiently using heterogeneous β-nucleating agents. Compared to the α-phase, the β-phase demonstrates significantly improved toughness and ductility but is thermodynamically less stable. When subjected to stretching at elevated temperatures, the β-phase can recrystallize into the α-phase [9–11]. The third crystalline phase of polypropylene is the orthorhombic γ-phase, which infrequently occurs under specific thermodynamic conditions [12], either through very high pressure [13, 14] or using types of material with low molecular weight, molecules with defects or copolymers [15].

Concerning polymorphic composition, long branches characterized by increased irregularities on the polymer backbone enhance PP's ability to crystallize into the orthorhombic γ-phase alongside the α-phase, even under elevated pressures [4]. Furthermore, the crystallization temperature significantly influences the regularity of helical conformation, thereby exerting a pronounced effect on the resulting crystalline phase structure of LCBPP [1]. The presence of branching points as structural defects hinders the rate of crystallite growth. Nevertheless, the overall crystallization process is accelerated in the case of LCBPP due to a significantly higher nucleating rate [6, 3].

Blending polymers is a proven and effective approach for creating novel polymeric materials featuring enhanced or tailored properties [16, 17]. This method not only lowers the expense associated with developing new polymers but also allows fine-tuning properties, such as substituting a portion of the composition with a more cost-effective polymer. In some instances, polymer blending is a more cost-effective alternative than using specific additives. It becomes feasible to tailor materials for targeted performances through adjustments in composition, blending conditions, and the introduction of chemical modifications or functional groups along the polymer chain, coupled with control of phase morphology. Polymer blending enables the optimization of rheological, mechanical, and thermal behaviors. LCBPP/PP blends have already been widely investigated. However, studies are mainly focused on the effect of the addition of long branches on the improvement of mechanical properties and rheological behavior of PP [3, 4, 18–27]. In the study of Stange *et al.* [21], it is assumed that the small number of long branches strongly affects long relaxation times and the strain hardening behavior at low strain rates. Thus, at least for polypropylene, low amounts of long branches lead to a similar strain rate dependence of the strain hardening, so the strain hardening decreases with increasing strain rate.

Furthermore, LCBPP can increase melt strength and enable a wider processing window of PP. Similar findings were observed by Fang *et al.* [23], who noted that adding LCBPP to PP improved melt strength, resulting in a strain-hardening behavior even at the 10% content of LCBPP. Moreover, McCallum *et al.* [24] found that PP/LCBPP blends exhibited increased melt strength and improved mechanical properties than PP.

According to the theory, the entanglement of long branching increases molecular interaction and decreases molecular slippage [25, 26]. As the result of the experiments of Zhao *et al.* [27], the long branches of LCBPP entangled as soon as formed, and the molecular weight of LCBPP was higher than that of PP. Moreover, spherulitic size is another essential factor affecting a material's impact strength. The higher nucleation rate and lower crystal growth rate of LCBPP promoted the formation of large numbers of small spherulites compared to PP. The size of PP's spherulites was larger than that of LCBPP, and the distribution of spherulites was lower than that of LCBPP; large but loose morphology results in more stress-concentrating points, which decreased the impact strength. Thermal analysis of blends from the study of McCallum *et al.* [24] revealed single melting and crystallization peaks for blends. The introduction of branched material significantly impacted both the melting and crystallization temperatures.

Tabatabaei *et al.* [28] found that for PPs with melt flow rate (MFR) values ranging from 4.0 to 0.4 g 10 min^{-1}, the incorporation of a small quantity (2.5 and 10 wt%) of LCBPP leads to an increase in nucleating sites, degree of crystallinity, and crystallization rate. However, with a higher proportion of branched material (40 and 60 wt%), a reduction in crystallinity content occurs, attributed to the constraint on chain mobility. Wang *et al.* [29] observed that the addition of 30 or 40 wt% of LCBPP resulted in increased nucleation and overall crystallization rates, along with elevated crystallization temperature. The study by Macedo *et al.* [30] focused on the evaluation of the rheological and thermal properties and non-isothermal crystallization kinetics of blends PP and LCBPP with the conclusion of possible application of the blends in processes demanding a combination of rheological properties, such as high strain hardening, and fast crystallization.

Although many studies have investigated LCBPP/PP blends, few are focused on the isothermal crystallization and polymorphic structure of the created blend. This study follows the previous study [19], which focused on the effect of nucleating agents on the crystallization of PP and LCBPP. The study aims to compare the effect of long-chain branching on the crystallization of PP during isothermal crystallization at various high crystallization temperatures (T_c). All blends containing different amounts of LCBPP are compared to the PP nucleated by a common sorbitol-based α-nucleating agent, targeted to find differences in nucleation efficiency in the selected range of various thermal crystallization conditions.

2. Experimental

2.1. Materials

Two distinct isotactic polypropylene grades were obtained from Borealis AG (Vienna, Austria). The first variety, Daploy WB140HMS, a long-chain branched polypropylene (LCBPP), exhibits a melt flow rate (MFR) of 2.1 g/10 min. This LCBPP possesses an isotacticity index of 96%, a weight-averaged molecular weight of 600 000 and a polydispersity index of 5.2. The second type, Borclean HC300BF, is linear polypropylene with an MFR of 3.3 g/10 min (both measured by ISO 1133, at 230 °C, 2.16 kg). This PP demonstrates an isotacticity index of 98%, a weight-averaged molecular weight of 300 000 and a polydispersity index of 8.0. In the case of LCBPP, the long branches were introduced into the primary polymer chain through monomer grafting via radical processes driven by peroxides in the molten state. Both polymers contain no process additives other than a standard stabilization system. Specific α-nucleating/clarifying agent Millad 3988 (1,3;2,4-bis(3,4-dimethylbenzylidene)sorbitol), supplied by Milliken Chemical, Ghent, Belgium, was applied in the concentration of 0.2 wt% in linear polypropylene [31].

2.2. Samples preparation

The nucleating agent (NA) was mixed into the PP in two steps, first manually, then using a twin-screw extrusion machine [19]. During the first step, 0.3 wt% of paraffin oil was added to the granulate to properly disperse NA Millad 3988 at the concentration of 0.2 wt%. Polypropylene blends containing 0.3% of paraffin oil and various amounts of LCBPP (1, 2, 5 and 10 wt%) and pre-mixed linear polypropylene with NA (PPN) were mixed by a co-rotating twin-screw extruder from Brabender GmbH & Co, Duisburg, Germany, including further cooling and pelletization processes. The extrusion conditions were established as followingly: a screw speed of 50 min^{-1}, with barrel zone temperatures set to 180, 200, and 210 °C. In order to ensure consistent processing and thermal treatment for all samples, neat PP and neat LCBPP underwent an identical procedure.

Subsequently, the prepared pellets were compression molded to produce plates with a thickness of 0.5 mm, using a pressing temperature of 210 °C for 5 min, followed by cooling at 60 °C for 10 min, as separators served polyethylene terephthalate films. The resulting specimens were subjected to wide-angle X-ray scattering (WAXS) and differential scanning calorimetry (DSC) to obtain information about the supermolecular structure and thermal properties of PP, LCBPP, nucleated PPN and blends. The nomenclature, along with the corresponding weight percentages of LCBPP incorporated into blends, can be found in Table 1.

2.3. Methods

The influence of varying amounts of LCBPP in blends compared to the influence of NA on the crystallization

Table 1. Nomenclature of blends.

	PP	**PPN**	**LCBPP**	**BL1**	**BL2**	**BL5**	**BL10**
LCBPP [%]	0	0.0	100	1	2	5	10
PP [%]	100	98.8	0	99	98	95	90
NA [%]	0	0.2	0	0	0	0	0

process of PP was investigated under isothermal conditions using a differential scanning calorimeter DSC1 by Mettler Toledo, Columbus, Ohio, USA. Samples, approximately 5 mg in weight, were loaded into aluminum pans and measured with an empty pan serving as a reference. Measurements were conducted within an inert nitrogen atmosphere at a gas flow rate of 20 ml/s.

The following thermal regime was applied: heating from 50 to 220 °C at a rate of 10 °C/min, annealing at 220 °C for 5 min to eliminate any prior thermal history, followed by cooling to crystallization temperatures (130, 135, 140, 142, 144, 146, 148 and 150 °C) at a cooling rate of 50 °C/min. Subsequently, the samples were held at the crystallization temperature until the crystallization peak was complete, but for no longer than 180 min. This was followed by heating to 190 °C by 10 °C/min to observe the melting profile.

The examination of the crystalline structure was carried out using a wide-angle X-ray diffractometer (PANalytical X'Pert PRO) from Malvern PANalytical, Malvern, United Kingdom. The diffractometer employed Bragg-Brentano geometry in reflection mode with CuKα radiation and a Ni filter (λ = 0.154 nm, I = 30 mA, U = 40 kV) within the diffraction angle range of 2θ = 5–30°. Additionally, a temperature cell (Anton Paar TCU 110, Graz, Austria) was incorporated into the diffractometer. Samples were prepared at dimensions of 10.0×14.0×0.5 mm to fit within the temperature cell, and conductive paste was utilized to ensure uniform thermal conductivity across the samples. The samples were then heated from 25 to 220 °C at a rate of 10 °C/min and held at this temperature for 5 min to obtain amorphous halo measurements.

Subsequently, the samples were cooled to the desired crystallization temperature, either 140 or 150 °C, based on the limit temperatures determined from DSC measurements, with a cooling rate of 20 °C/min. At this stage, the samples were maintained at the crystallization temperature for 171 min, and X-ray diffractograms were collected at specified intervals (0, 4, 8, 12, 99, 171 min) during the isothermal crystallization process. The crystallinity of the samples was calculated from the share of the fitted areas of the crystalline part (A_C) and amorphous part (A_A) using Equation (1) [32]:

$$X = \frac{A_\mathrm{A}}{A_\mathrm{C} + A_\mathrm{A}} \cdot 100\% \qquad (1)$$

X-ray patterns were analyzed by the Scherrer equation (Equation (2)), which gives the length L_hkl of the crystallite domain in the direction perpendicular to (hkl):

$$L_\mathrm{hkl} = \frac{K \cdot \lambda}{FWHM \cdot \cos 2\theta} \qquad (2)$$

where λ is the wavelength of the used X-ray, $FWHM$ is the full width at half maximum of the relevant peak, and 2θ is the peak position; both values are in radians. The constant K is omitted by setting it to 1, as in previous studies [19, 32].

3. Results and discussion

3.1. Thermal behavior

The DSC analysis compared the nucleation efficiencies of long branches and NA Millad 3389 and their impact on the crystallization process under isothermal conditions. Crystallization temperature varied from 130 to 150 °C, and crystallization time (t_c) was set to a maximum of 180 min. In the case of PP, the crystallization in the given time frame was completed only at low temperatures, 130 and 135 °C. At these low crystallization temperatures, the crystallization exotherms of LCBPP, PPN and all blends were incomplete because of the crystallization during cooling to the desired T_c. Figure 1 shows the comparison of crystallization curves of isothermally crystallized samples at various higher crystallization temperatures. Only the curves with whole exotherms are shown. Crystallization half-time calculated from the exotherms in Figure 1 is visible in Figure 2. The influence of long branches, acting as heterogenous nucleation seeds, is clearly visible. Neat PP exhibits whole crystallization at a given time frame only at lower crystallization temperatures (130 and 135 °C). With a rising amount of LCBPP content in the blends, the crystallization half-time shortens, which is the expected behavior compared to the crystallization of neat PP. LCBPP crystallizes fastest, even at the highest T_c. The effect of NA is visible; NA accelerates crystallization of more than 10% content of long branches but works only to T_c = 146 °C; at high temperatures, NA is not efficient, as was proved in a previous study [19]. In contrast, the long branches significantly support crystallization, and even with 1 wt% of LCBPP in the PP/LCBPP blend, the blend crystallizes up to the highest T_c. With higher concentrations of LCBPP, the differences in crystallization half-times decrease; the crystallization half-times of

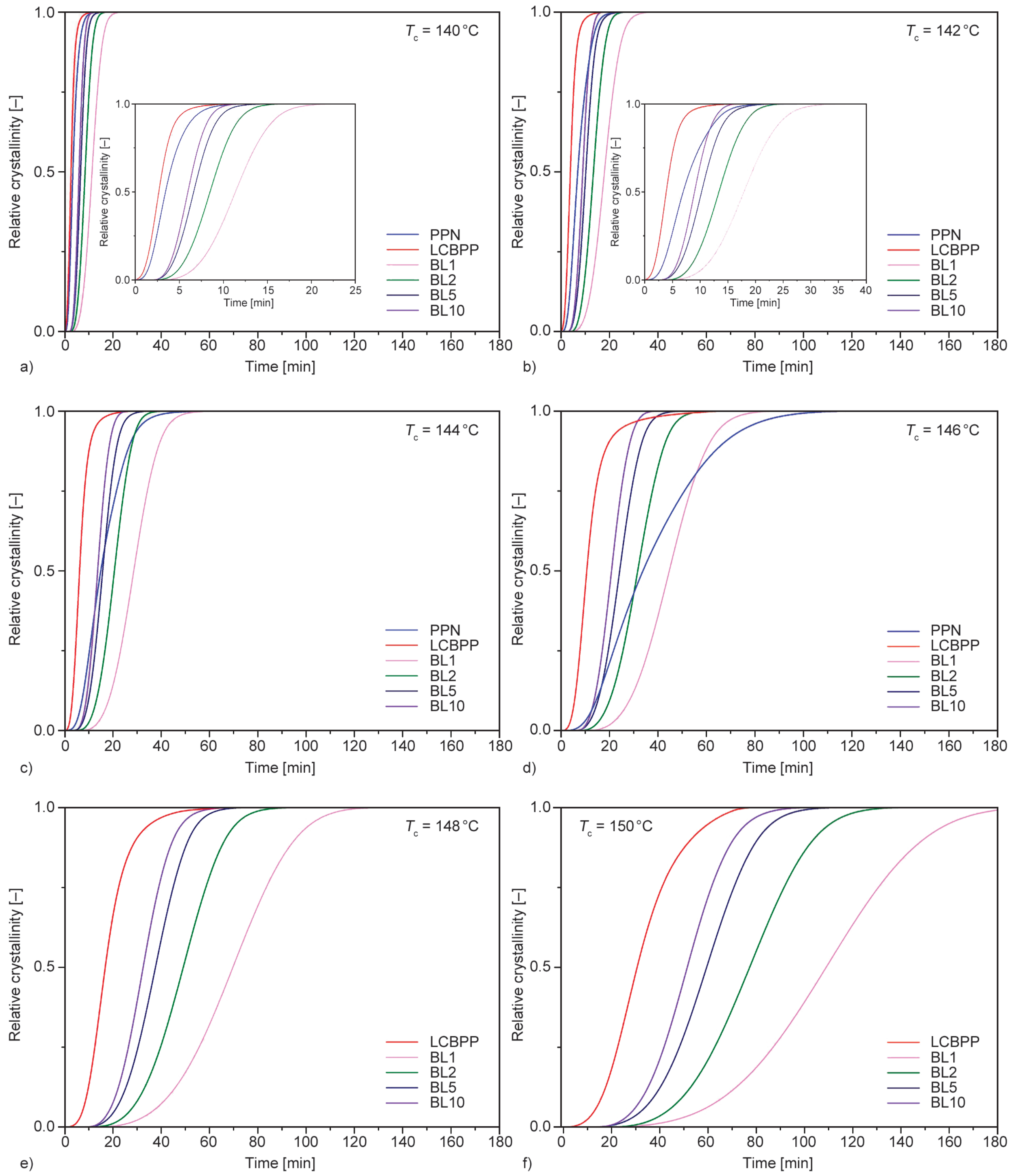

Figure 1. Crystallization curves of isothermally crystallized samples at various crystallization temperatures (the inset shows an x-axis cutout), a) T_c = 140 °C, b) T_c = 142 °C, c) T_c = 144 °C, d) T_c = 146 °C, e) T_c = 148 °C, f) T_c = 150 °C.

the blends become more similar, and if the blends were prepared at higher concentrations up to measured 100% LCBPP content, one would expect the crystallization half-times of these theoretical mixtures to be very similar to equal, indicating that higher concentrations do not affect significantly the rate of crystallization.

The isothermally crystallized samples were afterwards heated to obtain the melting temperature (melting temperature is the peak of the endotherm). The results are shown in Figure 3. In the case of neat PP, only the samples fully crystallized (at 130 and 135 °C) were melted, with visible melting temperatures of present dominating α-phase (approx. 167 °C) and

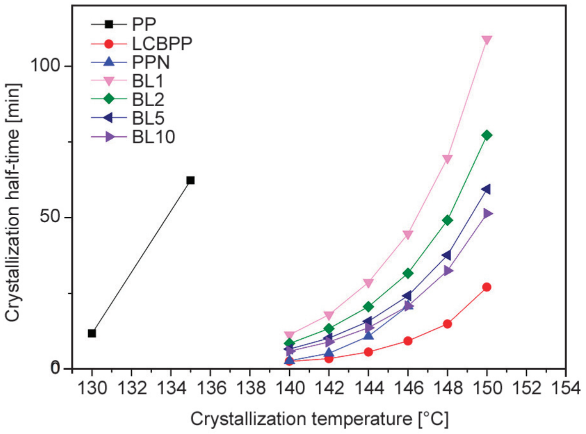

Figure 2. Crystallization half-time of samples crystallized at various crystallization temperatures.

small peak of β-phase (approx. 155 °C) for lower T_c. In general, the increase in melting temperature, depending on the increase of T_c, is observed. Two melting temperatures of PPN and blends refer to recrystallization of α_1-phase (approx. 170 °C) to more ordered α_2-phase (approx. 174 °C) during melting. The lower the value of melting temperature, the thinner the created lamellae structure. One can see that the thinnest lamellae of the α-phase have LCBPP. PPN and blends have similar melting temperatures, with the exception of BL1 reaching slightly lower values at higher crystallization temperatures. At T_c 130 and 135 °C, melting temperatures are similar to neat liner PP. However, no β-phase melting peak is observed as in the case of all blends. Thus, the addition of LCBPP into linear PP reduces the formation of β-phase during isothermal crystallization, playing the role of an α-nucleating agent.

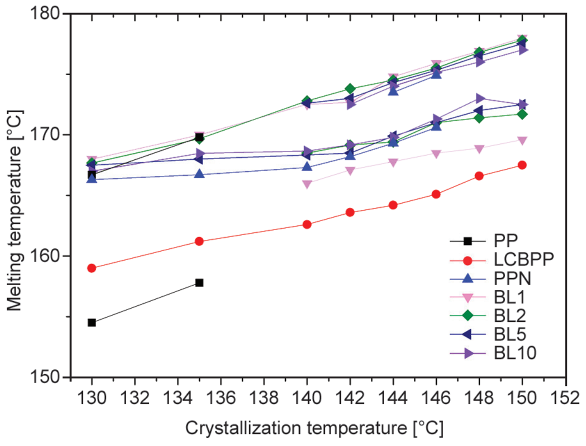

Figure 3. Melting temperatures of samples crystallized at various crystallization temperatures.

3.2. Supermolecular structure

Wide-angle X-ray Scattering (WAXS) in connection with a temperature cell was used to investigate the morphological characteristics of isothermally crystallized samples. Two crystallization temperatures, 140 and 150 °C, were selected as representatives based on outcomes derived from thermal analysis. The experimental procedure involved measurements carried out after the sample's melting, upon reaching the desired crystallization temperature, and at specified intervals during the crystallization process (0, 4, 8, 12, 99, and 171 min). Notably, the thermal conditions during WAXS differ from those during DSC due to variations in sample size, atmospheric conditions during measurements, and, predominantly, the cooling rate. Consequently, it is imperative to acknowledge that the results obtained from WAXS are not entirely comparable to those obtained from DSC, given the inherent differences in experimental conditions; however, the trends should be the same.

The presence of peaks corresponding to the main planes of the α-phase $\alpha_{(110)}$, $\alpha_{(040)}$, and $\alpha_{(130)}$, β-phase (300) and γ-phase (117) can be observed in the typical diffraction spectra of three-phase crystalline systems [6]. X-ray diffractograms of blends, presented in Figure 4, show the evolution of phases during isothermal crystallization at selected times. The progress of crystallization of neat PP, nucleated PPN and neat LCBPP was described in a previous study [19]; thus, these diffractograms are not presented here. The initiation of the crystallization process in neat PP isothermally crystallized at 140 °C occurred at crystallization time (t_c) 8 min of time-dependent crystallization. The final pattern (after t_c 171 min at 140 °C) contains, in addition to the α-diffraction peaks at angles 2θ = 14.20°, 17.00° and 18.80°, a small diffraction peak of the β-phase (16.20°) and also a small broad γ-phase diffraction peak (20.05°); a three-phase system with a dominant amount of α-phase was formed. The addition of NA to the PP significantly accelerated the crystallization process. Formation of the β-phase was suppressed entirely, while the diffraction peak corresponding to the γ-phase was observed; a two-phase α/γ system with α-phase dominance was formed. Increasing the crystallization temperature to 150 °C leads to a retardation of crystallization and also to the exclusive formation of the α-phase: no β- and γ-diffraction peaks

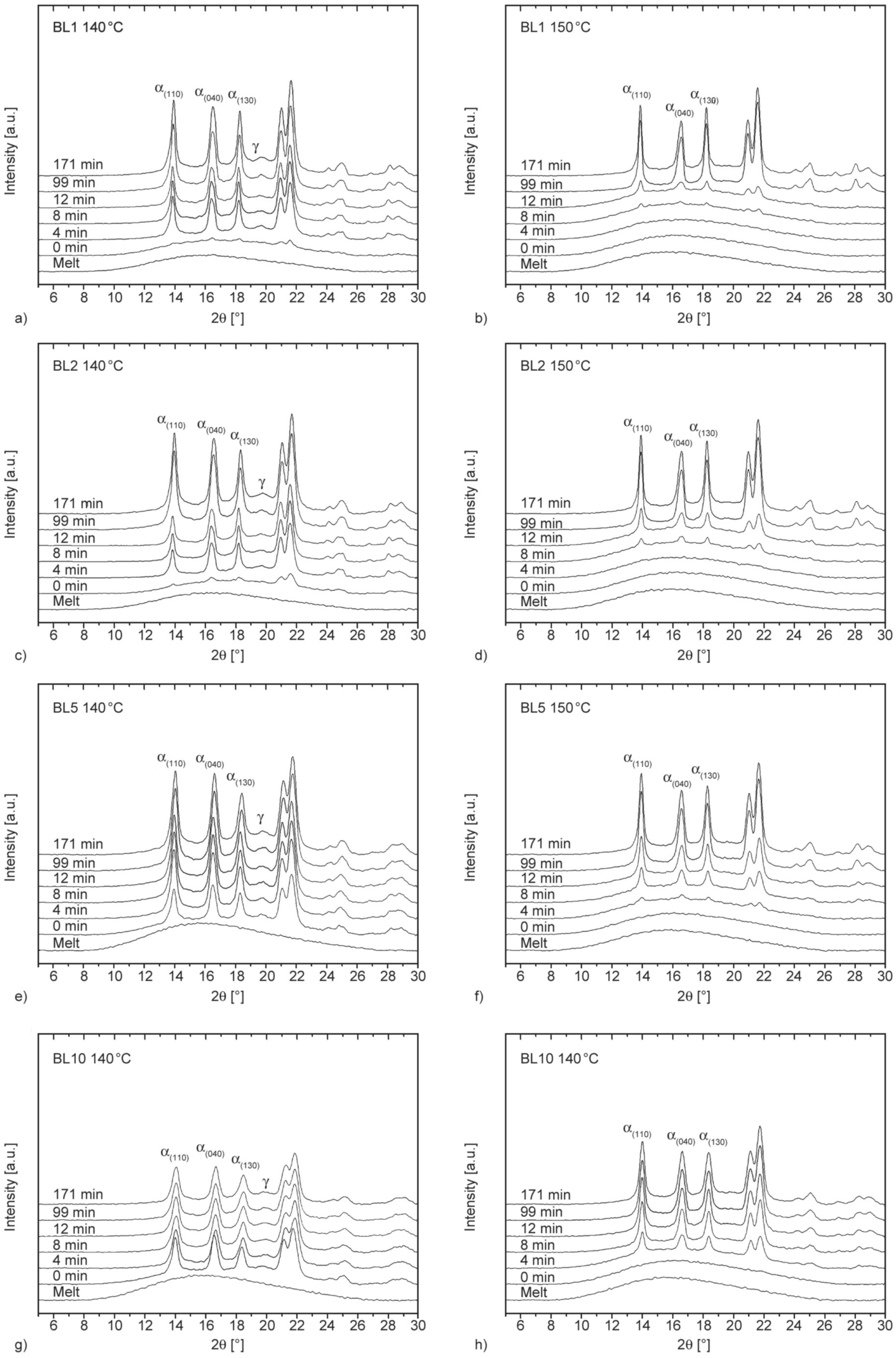

Figure 4. Evolution of WAXS patterns over time of crystallization a) BL1 at 140 °C, b) BL1 at 150 °C, c) BL2 at 140 °C, d) BL2 at 150 °C, e) BL5 at 140 °C, f) BL5 at 150 °C, g) BL10 at 140 °C, h) BL10 at 150 °C.

were observed. LCBPP crystallized into both the α- and γ-phases at 140 °C. At 150 °C, the crystallization was slightly slower, and the γ-phase diffraction peak disappeared.

With the rising amount of LCBPP content in the blends, the crystallization occurs faster, even at high T_c. It is visible that the γ-phase, at elevated T_c, disappears.

In Figure 5, overall crystallinity was calculated from the WAXS crystallization patterns (Figure 4) and plotted as a function of time. In the case of crystallization at 140 °C, except for neat PP, all samples crystallized partially upon cooling. Expectedly, LCBPP samples crystallize faster than nucleated PPN due to their self-nucleation ability, which is consistent with the DSC measurement results. The achieved overall crystallinity is higher for neat PP than for LCBPP. Adding an NA leads to a slight decrease in overall crystallinity, as does the addition of LCBPP independently on concentration. At 0 min, right after the desired T_c is reached, LCBPP possesses the highest overall crystallinity but remains almost the same after further crystallization. Although all blends were partially crystallized at 0 min, a plateau was reached at tc around 8 min and further, with slight differences. For higher T_c, 150 °C, the neat PP and nucleated PPN did not reach the plateau, so the final overall crystallinity could not be evaluated, but it is undoubtedly higher than in the case of LCBPP. When adding only 1% of LCBPP content into PP, overall crystallinity is higher than neat LCBPP, and the crystallization plateau is reached after 40 min of crystallization. Clearly, the addition of LCBPP into PP has, at an elevated T_c, a superior effect on the crystallization process, crystallization rate and overall crystallization than the addition of NA.

From the WAXS patterns obtained at the longest crystallization time, *i.e.* 171 min, by using the Scherrer equation, the values of the length L_{hkl} of crystallite domain in the direction perpendicular to (*hkl*) in the (110), (040) and (130) planes of the α-crystallites were calculated (Table 2). In the case of PP crystallized at 140 °C, adding the NA leads to a significant reduction in crystal dimension. However, this is not the case for a crystallization temperature of 150 °C; the dimension of the crystal remains the same, independent of the addition of NA; thus, at this high temperature, NA does not serve its function. Crystal

Table 2. Crystal dimension calculated from WAXS data.

Sample	T_c = 140 °C			T_c = 150 °C		
	L_{110} [nm]	L_{040} [nm]	L_{130} [nm]	L_{110} [nm]	L_{040} [nm]	L_{130} [nm]
PP	42.8	19.0	42.6	42.8	42.7	42.6
LCBPP	28.5	24.4	21.3	34.3	28.5	28.4
PPN	34.3	21.4	34.1	42.8	42.7	42.6
BL1	34.3	21.3	34.1	42.8	24.4	42.6
BL2	28.5	21.3	34.1	42.8	24.4	34.1
BL5	34.3	24.4	34.1	34.3	21.3	28.4
BL10	21.4	19.0	24.3	24.5	21.3	24.3

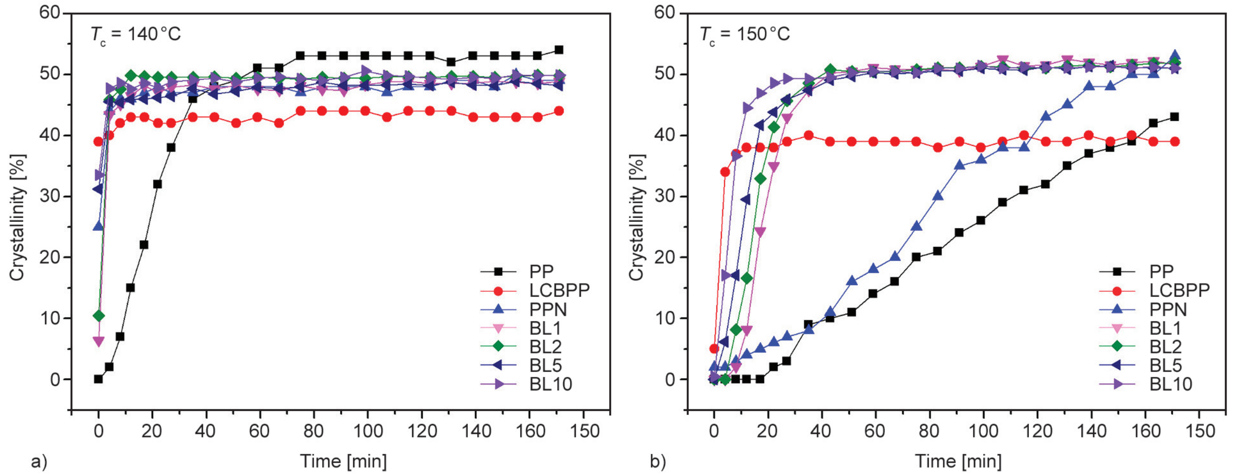

Figure 5. Growth of crystallinity during time-dependent isothermal crystallization at a) T_c = 140 °C and b) T_c = 150 °C.

dimension lowers with the rising amount of LCBPP. It can be noticed that at both crystallization temperatures, the blend with 10 wt% of LCBPP possesses a lower crystal dimension than neat LCBPP.

4. Conclusions

Based on the comparative study of the crystallization behavior and supermolecular structure of polypropylene blends incorporating various amounts of LCBPP and sorbitol-based clarifying NA Millad 3988 mixed into PP, this study provides valuable insights into the nucleating efficiency and crystallization kinetics of these systems. The results obtained from the thermal analysis reveal a clear advantage of LCBPP over NA in promoted crystallization, especially at elevated crystallization temperatures. While NA accelerates crystallization to a certain extent, its efficiency decreases at higher temperatures, whereas LCBPP consistently demonstrates superior nucleating ability across a range of temperatures. Incorporating LCBPP into PP blends enhances crystallization rates and overall crystallinity, indicating its effectiveness as a nucleating agent even at low concentrations. WAXS analysis clarifies the morphological evolution of the crystalline phases in the blends during isothermal crystallization. LCBPP facilitates the formation of α- and γ-phases, with the latter disappearing at elevated temperatures. Moreover, adding LCBPP leads to faster crystallization kinetics than nucleated PP, resulting in higher overall crystallinity.

The investigation into the crystal dimension using the Scherrer equation highlights the role of LCBPP in influencing the supermolecular structure. Blends with LCBPP exhibit shorter crystal dimensions than neat PP and nucleated PP, indicating finer crystalline structures and thus influencing physical properties [6, 19].

Overall, the findings underscore the significant impact of LCBPP as a nucleating agent on the crystallization behavior and supermolecular structure of PP blends.

Acknowledgements

The authors would like to thank project IGA/FT/2023/008 for financial support.

References

[1] Su Z., Wang H., Dong J., Zhang X., Dong X., Zhao Y., Yu J., Han C. C., Xu D., Wang D.: Conformation transition and crystalline phase variation of long chain branched isotactic polypropylenes (LCB-iPP). Polymer, **48**, 870–876 (2007). https://doi.org/10.1016/j.polymer.2006.12.013

[2] Nam G. J., Yoo J. H., Lee J. W.: Effect of long-chain branches of polypropylene on rheological properties and foam-extrusion performances. Journal of Applied Polymer Science, **96**, 1793–1800 (2005). https://doi.org/10.1002/app.21619

[3] Tian J., Yu W., Zhou C.: Crystallization kinetics of linear and long-chain branched polypropylene. Journal of Macromolecular Science Part B, **45**, 969–985 (2006). https://doi.org/10.1080/00222340600870507

[4] Navratilova J., Gajzlerova L., Kovar L., Cermak R.: Long-chain branched polypropylene: Crystallization under high pressure and polymorphic composition. Journal of Thermal Analysis and Calorimetry, **143**, 3377–3383 (2021). https://doi.org/10.1007/s10973-020-09931-1

[5] Auriemma F., Alfonso G. C., De Rosa C.: Polymer crystallization I.: From chain microstructure to processing. Advances in Polymer Science Vol. 276, Springer, Cham (2016).

[6] Gajzlerova L., Navratilova J., Ryzi A., Slabenakova T., Cermak R.: Joint effects of long-chain branching and specific nucleation on morphology and thermal properties of polypropylene blends. Express Polymer Letters, **14**, 952–961 (2020). https://doi.org/10.3144/expresspolymlett.2020.77

[7] Xu J., Reiter G., Alamo R. G.: Concepts of nucleation in polymer crystallization. Crystals, **11**, 304 (2021). https://doi.org/10.3390/cryst11030304

[8] Karger-Kocsis J.: Polypropylene: An A-Z reference. Kluwer, Dordrecht (1998).

[9] Mollova A., Androsch R., Mileva D., Gahleitner M., Funari S. S.: Crystallization of isotactic polypropylene containing beta-phase nucleating agent at rapid cooling. European Polymer Journal, **49**, 1057–1065 (2013). https://doi.org/10.1016/j.eurpolymj.2013.01.015

[10] Zhang C., Liu G., Song Y., Zhao Y., Wang D.: Structural evolution of β-iPP during uniaxial stretching studied by *in-situ* WAXS and SAXS. Polymer, **55**, 6915–6923 (2014). https://doi.org/10.1016/j.polymer.2014.10.049

[11] Bednarek W. H., Paukszta D., Szostak M., Szymańska J.: Fundamental studies on shear-induced nucleation and beta-phase formation in the isotactic polypropylene – Effect of the temperature. Journal of Polymer Research, **28**, 439 (2021). https://doi.org/10.1007/s10965-021-02652-5

[12] Mezghani K., Phillips P. J.: The γ-phase of high molecular weight isotactic polypropylene: III. The equilibrium melting point and the phase diagram. Polymer, **39**, 3735–3744 (1998).
https://doi.org/10.1016/S0032-3861(97)10121-5

[13] Maier C., Calafut T.: Polypropylene: The definitive user's guide and databook. Plastics Design Library, Norwich (1998).

[14] Mezghani K., Phillips P. J.: The γ-phase of high molecular weight isotactic polypropylene. II: The morphology of the γ-form crystallized at 200 MPa. Polymer, **38**, 5725–5733 (1997).
https://doi.org/10.1016/S0032-3861(97)00131-6

[15] Alamo R. G., Kim M-H., Galant M. J., Isasi J. R., Mandelkern L.: Structural and kinetic factors governing the formation of the γ polymorph of isotactic polypropylene. Macromolecules, **32**, 4050–4064 (1999).
https://doi.org/10.1021/ma981849r

[16] Tarashi S., Nazockdast H., Javidi Z., Mehranpour M.: Long-chain branch-induced interfacial interaction and its effect on morphology development in polypropylene/ethylene octene copolymer blend. Journal of Materials Science, **54**, 6742–6751 (2019).
https://doi.org/10.1007/s10853-019-03341-x

[17] Voges J., Juhre D.: Simulation of anisotropic diffusion under large deformations in polymer blends. Proceedings in Applied Mathematics and Mechanics, **18**, e201800320 (2018).
https://doi.org/10.1002/pamm.201800320

[18] Chvátalová L., Navratilova, J., Čermák R., Raab M., Obadal M.: Joint effects of molecular structure and processing history on specific nucleation of isotactic polypropylene. Macromolecules, **42**, 7413–7417 (2009).
https://doi.org/10.1021/ma9005878

[19] Zenzingerova S., Kudlacek M., Navratilova J., Gajzlerova L., Jaska D., Benicek L., Cermak R.: The competition between self-seeding and specific nucleation in crystallization of long-chain branched polypropylene. Express Polymer Letters, **17**, 1110–1120 (2023).
https://doi.org/10.3144/expresspolymlett.2023.84

[20] Auhl D., Stange J., Münstedt H., Krause B., Voigt D., Lederer A., Lappan U., Lunkwitz K.: Long-chain branched polypropylenes by electron beam irradiation and their rheological properties. Macromolecules, **37**, 9465–9472 (2004).
https://doi.org/10.1021/ma030579w

[21] Stange J., Uhl C., Münstedt H.: Rheological behavior of blends from a linear and a long-chain branched polypropylene. Journal of Rheology, **49**, 1059–1079 (2005).
https://doi.org/10.1122/1.2008297

[22] Langston J. A., Colby R. H., Chung M. T. C., Shimizu F., Suzuki T., Aoki M.: Synthesis and characterization of long chain branched isotactic polypropylene *via* metallocene catalyst and T-reagent. Macromolecules, **40**, 2712–2720 (2007).
https://doi.org/10.1021/ma062111

[23] Fang Y., Sadeghi F., Fleuret G., Carreau P. J.: Properties of blends of linear and branched polypropylenes in film blowing. The Canadian Journal of Chemical Engineering, **86**, 6–14 (2008).
https://doi.org/10.1002/cjce.20011

[24] McCallum T. J., Kontopoulou M., Park C. B., Muliawan E. B., Hatzikiriakos S. G.: The rheological and physical properties of linear and branched polypropylene blends. Polymer Engineering and Science, **47**, 1133–1140 (2007).
https://doi.org/10.1002/pen.20798

[25] Lee H. J., Goldberg M. J., Fetters J. L., Archer A. L.: Linear viscoelastic behavior of symmetric and asymmetric star polymer solutions. Macromolecules, **39**, 6677–6685 (2006).
https://doi.org/10.1021/ma061151a

[26] Deng S., Zhao X., Huang Y., Han X., Liu H., Hu Y.: Deformation and fracture of polystyrene/polypropylene blends: A simulation study. Polymer, **52**, 5681–5694 (2011).
https://doi.org/10.1016/j.polymer.2011.09.050

[27] Zhao W., Huang Y., Liao X., Yang Q.: The molecular structure characteristics of long chain branched polypropylene and its effects on non-isothermal crystallization and mechanical properties. Polymer, **54**, 1455–1462 (2013).
https://doi.org/10.1016/j.polymer.2012.12.073

[28] Tabatabaei S. H., Carreau P. J., Ajji A.: Rheological and thermal properties of blends of a long-chain branched polypropylene and different linear polypropylenes. Chemical Engineering Science, **64**, 4719–4731 (2009).
https://doi.org/10.1016/J.CES.2009.04.009

[29] Wang J., Jia H., Tang Y., Xiong X., Ding L.: Thermal stability and non-isothermal crystallization kinetics of metallocene poly(ethylene-butene-hexene)/high fluid polypropylene copolymer blends. Thermochimica Acta, **647**, 55–61 (2017).
https://doi.org/10.1016/j.tca.2016.11.016

[30] Macedo T. C. P., Campos D. A. T., Lima T. N., Rego J. K. M. A., Ito E. N., Ueki M. M.: Non-isothermal crystallization kinetics, thermal, and rheological behavior of linear/branched polypropylene blends. Macromolecular Symposia, **406**, 2200042 (2022).
https://doi.org/10.1002/masy.202200042

[31] Horváth Zs., Gyarmati B., Menyhárd A., Doshev P., Gahleitner M., Varga J., Pukánszky B.: The role of solubility and critical temperatures for the efficiency of sorbitol clarifiers in polypropylene. RSC Advances, **4**, 19737–19745 (2014).
https://doi.org/10.1039/c4ra01917b

[32] Gajzlerova L., Navratilova J., Zenzingerova S., Jaska D., Benicek L., Kudlacek M., Cermak R., Obadal M.: On isotactic polypropylene annealing: Difference in final properties of neat and β-nucleated polypropylene. Express Polymer Letters, **16**, 453–464 (2022).
https://doi.org/10.3144/expresspolymlett.2022.34